# Surface Characterization and Adhesive Properties of Poly(imidesiloxane) Copolymers Containing Multiple Siloxane Segment Lengths

**Christine M. Mahoney and Joseph A. Gardella, Jr.***

*Department of Chemistry, University at Buffalo, SUNY, Buffalo, New York 14260-3000*

**Jerold C. Rosenfeld**

*Occidental Chemical Corporation, Grand Island, New York 14072*

*Received February 26, 2001; Revised Manuscript Received January 31, 2002*

ABSTRACT: A series of poly(imidesiloxane) (SIM) copolymers have been synthesized from α,ω′-aminopropylpoly(dimethylsiloxane) (PDMS) of varying lengths, 2,2-bis(4-[4-aminophenoxyl]phenyl)propane (BAPP), and 4,4′-oxydiphthalic anhydride (ODPA). In this series, the total composition of PDMS was maintained at 10 wt % with multiple PDMS segment lengths of different relative compositions (e.g., 5% PDMS containing 1 repeat unit, designated G-1, and 5% PDMS containing an average repeat unit of 9, designated G-9, incorporated into the same polymer vs 1% G-1 and 9% G-9 in the same polymer). Two main polymer series were synthesized: one containing G-1 and G-9 in varying ratios and the other containing G-5 and G-9. Both of these series have been analyzed using angle-dependent X-ray photoelectron spectroscopy (XPS). The Si/N ratios as measured by XPS from all members of the G-9/G-1 series were statistically equivalent to that of the polymer containing pure 10% G-9, while that of the polymer containing 10% G-1 had a significantly lower value. This suggests that there is preferential segregation of the longer G-9 siloxane segment lengths to the surface. These same studies were repeated for the series containing both G-5 and G-9, and similar results were found, although the extent of segregation was less. The angle-dependent data were then used to obtain an in-depth profile by using a numerical algorithm, which was designed for samples with compositional gradients as is the case with this system. From the profiles, it was determined that the thickness of the surface PDMS layer of all polymers containing both G-9 and G-1 was the same for all compositions studied, while that of the pure 10% G-1 was much thinner. The adhesion strengths of these polymers were measured using peel strength tests, and the adhesion values were correlated to the XPS results. It was found that the adhesion of the pure 10% G-1 was much higher than that of any other polymer in the series. The remainder of the polymers in the series all had similar adhesion values. These results are consistent with a model of the surface, which has longer segment lengths preferentially segregating and dominating the adhesive properties.

## Introduction

Poly(imidesiloxane) (SIM) copolymers are becoming increasingly important materials for microelectronic applications primarily due to their excellent adhesive properties, low dielectric constants, and good overall thermal and mechanical properties. These copolymers have already been employed for use as die-attach adhesives, protective coatings, interlayer dielectrics, and encapsulents.[1−4] With the combined properties of the polyimide and poly(dimethylsiloxane) (PDMS) components, SIM copolymers have increased solubility and flexibility as compared to the polyimide homopolymer, leading to increased overall processability. The introduction of the siloxane component allows for increased impact resistance, excellent adhesion, reduced water absorption, decreased dielectric constants, and increased gas permeability, while maintaining the thermal and mechanical stability that is adequate for most microelectronic applications.[4,5]

Poly(imidesiloxane) block copolymers, however, are much more complicated than the polyimide homopolymers in that there are two components involved, which have a low mixing entropy. This low mixing entropy results in microphase separation of the polymer, with a domain size that varies with block length and percentage of PDMS. Also, in copolymer systems, the low surface energy component (in this case PDMS) will tend to migrate to the surface in order to minimize the total free energy of the system. Numerous studies have shown that the PDMS tends to microphase separate and segregate to the surface in copolymer systems. PDMS has been shown to predominate in the surface of such block copolymers as polystyrene (PS−PDMS),[6−8] bisphenol A polycarbonate (BPAC−PDMS),[8−12] poly(methyl methacrylate) (PMMA−PDMS),[13] nylon-6−PDMS,[14] polyurethane (PU−PDMS),[15,16] and many other copolymer systems.[17−25] This phenomenon has also been shown to occur in poly(imidesiloxane) copolymer systems.[21−25] The extent to which this segregation occurs, however, depends on numerous variables including bulk composition, block length, processing conditions (such as annealing and casting solvent), and the block sequence distribution. For example, Zhao et al.[23] used X-ray photoelectron spectroscopy (XPS) to show that increasing the segment length of the PDMS block, while maintaining the same overall bulk content of PDMS (10%), resulted in a significant increase in the content of PDMS at the surface. It was also shown that while changing the PDMS segment lengths changed the surface characteristics of the copolymer, changing the total bulk concentration of PDMS incorporated into the polymer did not significantly alter the extent of siloxane segregation to the surface. Further studies involving

* To whom correspondence should be addressed. E-mail: gardella@acsu.buffalo.edu.

10.1021/ma010353y CCC: $22.00 © 2002 American Chemical Society
Published on Web 05/24/2002

XPS depth profiling showed that increasing the segment length actually resulted in an increase in the thickness of the PDMS surface layer.[24] These properties were correlated with the adhesion characteristics of the polymer through peel strength testing, and it was found that the longer siloxane segment length polymers containing a thicker PDMS layer at the surface had poorer adhesion.

Many other studies have been done relating the surface properties of poly(imidesiloxane)s to the adhesion properties.[25−29] In studies done by Yoon et al., adhesion testing via single lap shear was done on polyimides of varying molecular weights and percentages of siloxane to determine what conditions would result in optimal adhesion. It was found through these studies that the adhesion increased with increasing siloxane content up to 20% when tested at room temperature.[26] One might expect that the adhesion would decrease upon the addition of siloxane to the polymer, since the siloxane has a much lower surface energy and is not involved in the actual adhesion mechanism. The enhanced adhesion results from the increased flexibility and ductility that the polymer obtains through the addition of PDMS, which allows for intimate contact of the imide groups with the substrate in question.

Zhuang et al. performed XPS on the surface of poly(imidesiloxane) after it had been peeled from a Ni/Fe alloy surface and found a 4-fold increase in the amount of nitrogen at the peeled interface than at the air interface.[25] This further confirms that it is the imide portion of the copolymer that is involved in the adhesion process. Spectra were taken on the surface of the alloy after peeling as well. There was a detectable amount of N at the surface, suggesting that the failure that occurred during peel testing was cohesive rather than adhesive.

To our knowledge, no one has studied the effect of incorporating two or more different PDMS blocks lengths into the same polymer on the surface characteristics. In this project, a new polymer series containing two different short segment lengths of PDMS in a single polymer has been synthesized and characterized by XPS.[30,31] The adhesion of this series was measured through peel strength testing in order to correlate the adhesion strength to its surface properties. It is of special interest to determine whether there is preferential segregation of certain siloxane segment lengths to the surface and the effects this may or may not have on the adhesion strength of the polymer. Poly(imidesiloxanes) can be used as a model system to study the surface structure/property relationships of copolymers containing PDMS. It is important to remember that these studies, however, are focused on shorter PDMS segment lengths (MW < 1000 g/mol). The results discussed in the present study may differ for longer PDMS segment lengths (MW > 1000 g/mol), as there are different thermodynamic driving forces involved.

## Experimental Section

**Sample Preparation.** The poly(imidesiloxane)s discussed in this paper have been synthesized from the flexible aromatic dianhydride, ODPA (ChrisKev, Leawood, KS), the rigid aromatic diamine, BAPP (ChrisKev, Leawood, KS), and α,ω′-aminopropylpoly(dimethylsiloxane) (PCR Inc., Gainsville, FL) of varying molecular weights. ODPA was chosen because it gives good solubility, while the BAPP was chosen simply for its low cost and low toxicity.[32] The sample preparation is outlined in Scheme 1. First, the PDMS was added, with stirring, to a solution containing BAPP in 1-methyl-2-pyrolidinone (NMP) and toluene in a 4 to 1 ratio. This mixture of NMP and toluene was used in order to ensure that both PDMS and polyimide components were soluble in the final solution. The ODPA was added slowly to this mixture, initiating the reaction. The mixture was then left to react for 16−20 h with stirring in order to ensure a complete reaction. The resultant polyamic acid was either spin-coated onto aluminum or drawn by a doctor blade onto a Teflon sheet and imidized in a Fisher Scientific Isotemp programmable oven (model 838F) at a series of temperatures. The first temperature was set at 120 °C for 1 h in order to ensure that there was adequate solvent removal. The temperature was then ramped up to 250 °C with a ramp rate of 7 °C/min and held at 250 °C for 1 h in order to allow for the completion of the imidization process. Samples used for analysis in the XPS chamber were spin-coated onto Al substrates, while samples used for peel strength testing involved the use of the doctor blade (rpm used for spin-coating varied with the viscosity of the polyamic acid). The thickness of the polymer films varied between samples but tended to be around 60−100 μm for the doctor blade-cast films and ≤5 μm for the spin-cast films.

**Table 1. Table of Poly(imidesiloxane)s**

| name | siloxane composition | $T_g$ | CTE | $M_N$/PI |
|---|---|---|---|---|
| A | 1% G-1 | | | |
| B | 5% G-1 | | | |
| **C** | 10% G-1 | 158.3 ± 2.0 | 81.0 ± 1.9 | 36137/1.63 |
| D | 20% G-1 | | | |
| E | 30% G-1 | | | |
| F | 1% G-9 | | | |
| G | 5% G-9 | | | |
| **H** | 10% G-9 | 185.4 ± 0.7 | 101.9 ± 9.9 | 54103/2.06 |
| **H**[a] | 10% G-9 | 183.8 ± 0.4 | 109.6 ± 16.01 | |
| I | 20% G-9 | | | |
| J | 30% G-9 | | | |
| **K** | 9% G-9, 1% G-1 | 182.6 ± 0.46 | 101.5 ± 18.5 | 74898/2.06 |
| **L** | 7% G-9, 3% G-1 | 178.2 ± 1.0 | 100.2 ± 6.3 | 68640/1.97 |
| **M** | 5% G-9, 5% G-1 | 172.4 ± 0.9 | 102.6 ± 9.9 | 76005/2.10 |
| **N** | 3% G-9, 7% G-1 | 166.8 ± 0.7 | 88.7 ± 2.3 | 130710/1.35 |
| **O** | 1% G-9, 9% G-1 | 162.5 ± 0.3 | 104.3 ± 11.7 | 156320/1.44 |
| P | 10% G-3 | 166.9 ± 0.3 | 92.8 ± 10.1 | |
| **Q** | 10% G-5 | 176.1 ± 0.4 | 102.2 ± 2.0 | 86602/1.91 |
| **Q**[a] | 10% G-5 | 171.7 ± 0.4 | 113.7 ± 18.8 | |
| R | 10% G-7 | 181.6 ± 1.8 | 97.3 ± 8.6 | 46040/1.7 |
| S | 3.3% G-1, 3.3% G-3, 3.3% G-5 | | | |
| **T** | 3.3% G-7, 3.3% G-9, 3.3% G-12 | | | |
| U | 10% G-12 | 194.2 ± 0.5 | 109.8 ± 14.7 | 60817/1.87 |
| V | 3.3% G-1, 3.3% G-5, 3.3% G-12 | | | |
| **W$_a$**[a] | 9% G-5, 1% G-9 | 182.1 ± 0.2 | 107.6 ± 14.1 | |
| **W$_b$**[a] | 7% G-5, 1% G-9 | 180.4 ± 1.3 | 104.3 ± 5.9 | |
| **W$_c$**[a] | 5% G-5, 1% G-9 | 177.9 ± 0.9 | 104.2 ± 10.4 | |
| **W$_d$**[a] | 3% G-5, 1% G-9 | 176.8 ± 0.2 | 105.6 ± 8.9 | |
| **W$_e$**[a] | 1% G-5, 1% G-9 | 174.4 ± 0.5 | 96.6 ± 9.2 | |
| $A_2$ | 2% G-1 | | | |
| $Q_2$ | 2% G-5 | | | |
| $F_2$ | 2% G-9 | | | |
| $M_2$ | 1% G-1, 1% G-9 | | | |
| $W_2$ | 1% G-5, 1% G-9 | | | |
| Z | no PDMS | | | |

[a] Samples prepared on a different day.

The series of polymers synthesized are listed in Table 1. However, we will only be discussing the boldfaced polymers here. PDMS with average molecular weights ($M_N$) of 252, 440, 550, 703, 833, and 1180 g/mol were incorporated, corresponding to $p$ values (PDMS segment lengths) of 1, 3, 5, 7, 9, and 12, respectively (see Scheme 1). These different segment lengths are denoted as G-$X$, where $X$ represents the $p$ value in the reaction scheme (e.g., PDMS with an average segment length of 9 is referred to as G-9). This notation is used simply because it is the notation used by PCR Inc. to describe the length of the siloxanes. Polymers C, P, Q, R, H, and U are a

**Scheme 1. Reaction Scheme for Synthesis of Poly(imidesiloxane)[a]**

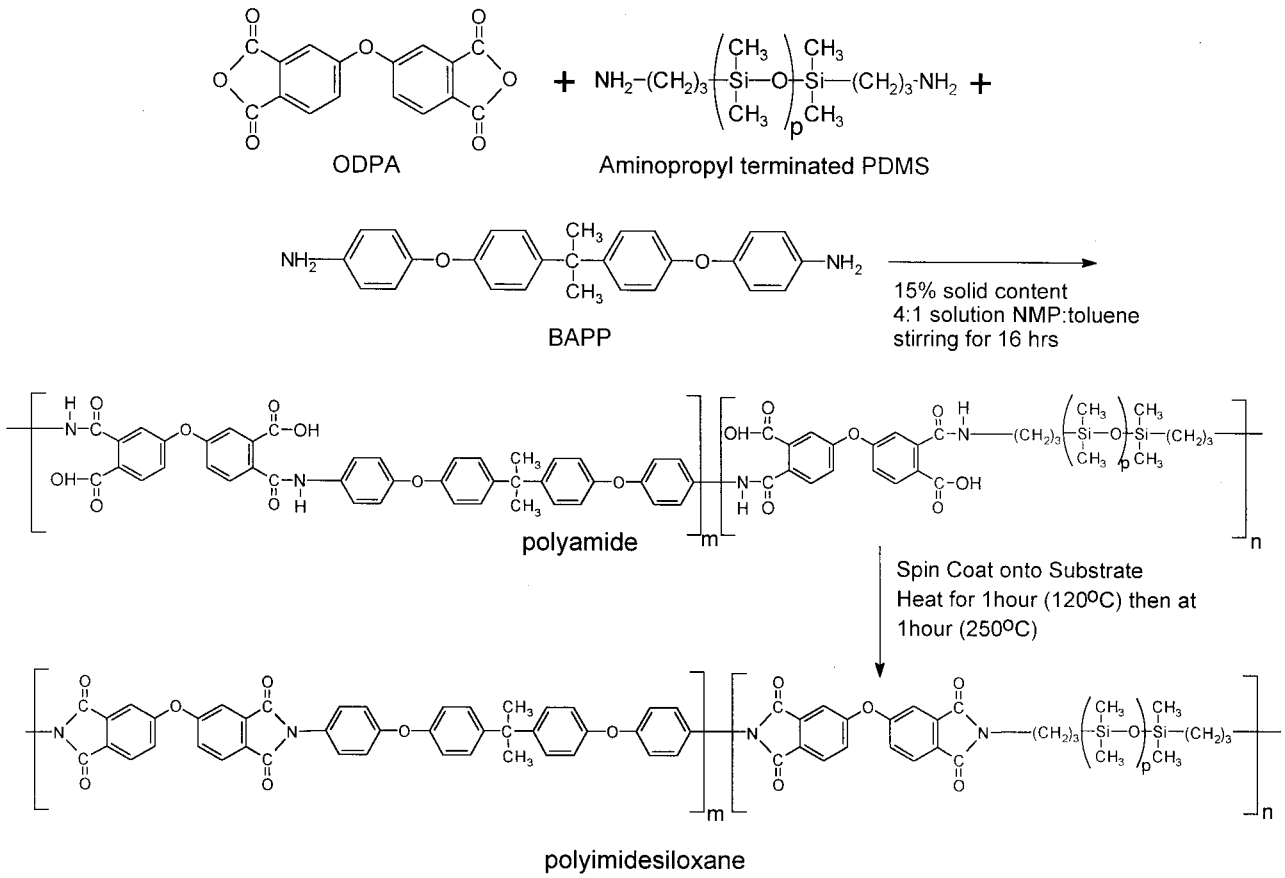


[a] The stoichiometric ratio of the reactants determines the composition of the final product. Increasing the ratio of PDMS/BAPP will result in an increase in the total weight percentage PDMS. This ratio can be maintained while varying the segment length(s) of PDMS used to get varying segment lengths in the final product.

series of polymers that contain different segment lengths, while maintaining a constant weight percentage of 10% overall siloxane. Different block compositions can result from varying the ratio of *m*/*n* in Scheme 1. The larger the ratio of *m*/*n*, the smaller the percentage of siloxane incorporated in the polymer. Polymers A−E contain varying G-1 percentages, and polymers F−J contain varying G-9 percentages. These polymers have already been characterized.[23,24] In the present work, two different siloxane segment lengths (G-1 and G-9) were incorporated into the same polymer chain. In this series (polymers K−O from Table 1), the total composition of PDMS was maintained at 10%, while the segment length composition of the PDMS was varied (e.g., 5% G-1, 5% G-9 vs 1% G-1, 9% G-9). A similar series containing varying compositions of G-5 and G-9 were also synthesized ($W_a$−$W_e$). This series was characterized in a similar manner.

All polymers were cleaned with toluene in order to extract any unreacted low molecular weight PDMS from the polymer. This is important, as this PDMS will migrate to the surface and form a weak boundary layer, which will inhibit adhesion. The samples used in XPS measurements were sonicated in toluene for 2 min, while those involved in adhesion testing were sonicated for 5 min. The longer sonication times associated with the adhesion samples is attributed to the fact that the samples used for adhesion testing had much greater surface areas and were much thicker than the films that were used for XPS analysis.

**XPS.** XPS studies were performed on a Physical Electronics/PHI 5300 X-ray photoelectron spectrometer with a hemispherical analyzer and a single channel detector, operated at 300 W (15 kV and 20 mA). Mg Kα radiation (1253.6 eV) and pass energies of 89.45 eV for survey scans and 17.9 eV for high-resolution scans were used for all work. The base pressure was maintained at approximately $1 \times 10^{-8}$ Torr. Signals from all four detectable elements in poly(imidesiloxane) were analyzed for carbon, nitrogen, oxygen, and silicon, and the binding energies were calibrated by setting C 1s at 285 eV. Angle-dependent XPS work has been performed on these samples, where the sampling depth is defined as $d_s = 3\lambda \sin \theta$ ($\lambda$ = escape depth of the photoelectrons, $\theta$ = photoelectric takeoff angles). Hence, as we increase the photoelectric takeoff angle, we are also increasing the sampling depth. All angle-dependent work was performed at takeoff angles of 10°, 15°, 30°, 45°, and 90°. The atomic sensitivity factors (ASF) used for quantification are relative to F 1s = 1.00. The ASF's used in this work are 0.27 for Si 2p, 0.42 for N 1s, 0.66 for O 1s, and 0.25 for C 1s.[33,34] The atomic concentration of each element was obtained from the XPS signal area divided by the corresponding ASF.

**Calculations of In-Depth Profiles.** The depth information obtained by angle-dependent XPS is not a direct measure of the composition as a function of depth. All atoms within the path of the probing X-ray will contribute to the signal, but the contribution of each will decrease exponentially with the distance from the free surface. This is because electrons released deeper into the sample are less likely to reach the detector as a result of the limitations of scattering and energy loss in the solid. Hence, the spectra obtained will be convoluted in a manner that will be more representative of the very surface, rather than deeper into the bulk. This is summarized by the following general intensity relationship:

$$I_i = \int_0^\infty I_i(x) e^{(-x/\lambda_i)}\, dx \qquad (1)$$

where $I_i$ is the detected intensity of photoelectrons from a given atom $i$, $x$ is the vertical distance from the free surface, and $\lambda_i$ is the mean free path of electrons from atom $i$. Keep in mind that this equation describes a situation where the takeoff angle is constant. To obtain depth profile information, measurements

must be taken at multiple angles. The intensity relationship thus becomes

$$I_i(\theta) = F\alpha_i K \int N_i(x) e^{-x/(\lambda_i \sin\theta)}\, dx \qquad (2)$$

where $\theta$ is the photoelectron takeoff angle, $F$ is the X-ray flux, $\alpha$ is the cross section of photoionization in a given shell of a given atom for a given X-ray energy, $N(x)$ is the depth profile of the atomic density, and $K$ is a spectrometer factor.

To obtain accurate depth profiles, the convolution of the XPS data must be accounted for. Previous reports from our laboratory have described a method of recovering depth profile information using angle-dependent XPS data, which is based on a numerical algorithm.[16,24,35−37] Unlike most methods involving the use of algorithms to recover depth profile information, this method was designed for samples with compositional gradients, as is common with many copolymer systems. The basic theory behind XPS depth profile recovery is outlined below in a similar fashion as refs 16 and 24. C/N ratios, rather than C/Si ratios, were used in previous calculations due to larger variations in the nitrogen concentration at different sampling depths.[16] These equations were developed for systems in which the major constituent was silicon (at least 70%).[16] In our case, however, Si is the minor constituent making up only 10% of the total polymer weight. Hence, these equations have been modified in order to obtain more accurate results. They have also been modified to allow for calculations involving five angles, rather than four. However, these results will not be shown as the 10° angle actually adds more error to the final profile. This increase in error at the 10° angle is attributed to the decreased efficiency of the lenses at angles lower than 15°, resulting in decreased signal-to-noise ratios and also to the fact that an extremely small amount of N is detected at this angle.

The intensities of the photoelectron response from carbon and silicon as a function of takeoff angle can be formulated in the derivative form as follows:

$$dI_{Si}(\theta) = F\alpha_{Si} N_{Si}(x) K e^{-x/(\lambda_{Si} \sin\theta)}\, dx \qquad (3)$$

$$dI_{C}(\theta) = F\alpha_{C} N_{C}(x) K e^{-x/(\lambda_{C} \sin\theta)}\, dx \qquad (4)$$

where subscripts Si and C denote silicon and carbon, respectively. The inelastic mean free paths as calculated by the modified Bethe equation for C and Si are approximately 19 and 21 Å, respectively.[37] An average value of 20 Å will be used for the purpose of this study. Assuming $F$, $K$, and $\alpha$ are independent of $x$ and defining the normalized intensity $I'(\theta)$ as $I(\theta)/(F\alpha K)$, one can integrate eqs 3 and 4 to give the following equations:

$$I_{Si}'(\theta) = I_{Si}(\theta)/(F\alpha_{Si}K) = \int N_{Si}(x) e^{-x/(\lambda_{Si} \sin\theta)}\, dx \qquad (5)$$

$$I_{C}'(\theta) = I_{C}(\theta)/(F\alpha_{C}K) = \int N_{C}(x) e^{-x/(\lambda_{C} \sin\theta)}\, dx \qquad (6)$$

To recover these depth profiles, it is necessary to first define atomic density profiles ($N_C$ and $N_{Si}$). The polymer chains were first divided into hard and soft segments. In this case, the hard segment is the polyimide segment ($m$ in Scheme 1), while the soft segment is the PDMS portion of the polymer ($n$ in Scheme 1). Assuming that the changes in density throughout the film and the difference between weight fraction and volume fraction are negligible, the atomic depth profile for C and Si are as follows:

$$N_C(x) = \sigma v + \eta(1 - v) \qquad (7)$$

$$N_{Si}(x) = \sigma v \gamma \qquad (8)$$

where $\eta$ and $\sigma$ are the carbon densities for the hard segment and the soft segments, respectively, $\gamma$ is the silicon-to-carbon ratio in the soft segment, and $v(x)$ is the nonconvoluted depth profile of the soft segments. $\eta$, $\sigma$, and $\gamma$ are dependent on the structure of the poly(imidesiloxane) and the type of PDMS incorporated. $v(x)$ is the profile of interest. Once defined, eqs 7 and 8 can be solved and plugged into eqs 5 and 6 to obtain a calculated C-to-Si ratio. This value is then compared to the experimental ratios, whereupon the profile is modified to obtain maximum agreement between the two ratios. Hence, this is really not a "deconvolution" process, where the XPS data are deconvoluted to obtain a profile, but a process involving the convolution of a theoretical profile and comparison of the results to experimental data.

The method of determination of $v(x)$ involves the use of two models previously described as the discrete model and the continuous model.[16] The discrete model allows for an approximation of $v(x)$ as the sum of nine step functions. Each step function staggers the previous one by a certain distance $l$, where $l$ is optimized by refining sequential fits. By continual adjustment of the height ($h$) of the step functions, a depth profile can be obtained that gives atomic concentrations that are consistent with the XPS data. The discrete model is used to approximate the type of function that best describes the surfaces of these copolymer systems. A basis for a starting point can be determined on the basis of polymer composition. However, a continuous function is desirable for obvious reasons. Because the functions described by the discrete model have a minimum in our case, a Gaussian distribution model with four parameters was chosen as a model to determine $v(x)$. This function is shown in eqs 9 and 10:

$$v(x) = C_{bulk} H \exp[0.5(l^y - L)^2/S_1^2] \qquad l < L \qquad (9)$$

$$v(x) = C_{bulk}\{(H - 1) \exp[-0.5(l - L)^2/S_2^2]\} \qquad l > L \qquad (10)$$

where $C_{bulk}$ is the volume fraction (weight fraction) of PDMS segments in the bulk, which is in our case 0.1, $H$ is the $y$ axis value at the minimum of the profile, $l$ is the distance from the surface, $L$ is the location of the minimum of the profile, $S_1$ characterizes the shape of the profile to the left of the minimum, and $S_2$ characterizes the shape of the profile to the right of the minimum. To make an appropriate fit to the discrete model, eq 9 has been modified slightly from previous studies such that the negative exponent was changed to a positive value and a $y$ exponent was added. The negative sign in the exponent was removed because we are looking at a decrease in Si concentration, rather than the increase in N signal, which has been described in previous work. The $y$ exponent was added in order to change the onset of the drop in the profile so that it better fit the results from the discrete model. Before the $y$ exponent was added, the curve showed exponential decay, which does not accurately describe the results from the discrete model. The value for this $y$ has been determined by matching the continuous and discrete models and has been determined to be 3 for the polymer containing G-1 only and 7 for all others. Equation 10 was not changed as it described the curves accurately for both cases.

Once $v(x)$ is defined, eqs 7 and 8 (atomic density profiles for C and Si) can be solved. These profiles are then be placed into eqs 5 and 6, where $I'_C/I'_{Si}$ is determined. If the calculated data match the experimental data, then the profile is kept. To reach optimal values of these four parameters, the following objective function based on the Gauss−Newton method was used:

$$\psi = \{(1/n)\sum[R_{cal}(H,L,S_1,S_2) - R_{exp}(\theta_n)]/[R_{exp}(\theta_n)]^2\}^{1/2} \qquad (11)$$

where $n$ is the number of takeoff angles which is four in this case, $R_{cal}$ is the ratio of intensities of C to Si as calculated by the continuous model, and $R_{exp}$ is the experimental ratio of intensities. The starting values for the optimization procedures were obtained by scanning the five-dimensional space. A grid was imposed on the $(H,L,S_1,S_2)$ space, $\psi$ values at selected intersections were calculated, and the coordinates of the location where the minimum was found were used as the starting values. The process is repeated with the new values

**Table 2. Parameters Used in the Calculations for ESCA Deconvolution and the Resultant Error**

| polymer | $C_{bulk}$ | $\eta$ | $\sigma$ | $\gamma$ | $H$ | $L$ | $S_1$ | $S_2$ | $\Psi$ |
|---|---|---|---|---|---|---|---|---|---|
| C | 0.1 | 61.70 | 46.30 | 0.200 | 0.504 | 0.22 | 0.94 | 0.32 | 0.022 |
| H | 0.1 | 62.74 | 32.18 | 0.385 | 0.138 | 0.7 | 0.239 | 2.00 | 0.015 |
| K−O | 0.1 | 62.74 | 32.18 | 0.385 | 0.130 | 0.699 | 0.24 | 1.082 | 0.006 |

until the lowest possible $\psi$ is reached. Table 2 shows the results of minimizing $\psi$.

**Adhesion Testing.** Adhesion testing was done primarily on a Diventro peel tester adapted with a 5 kg Omega digital force gauge connected to a strip chart recorder. The polymer films prepared with the doctor blade were used for this test. The films were first cut into strips, $^1/_4$ in. × 2 in. (6.3 mm × 50 mm) in width. These strips were then melt-cast onto clean Ni/Fe alloy 42 substrates (cleaned by soaking in a degreaser (Bioact) for at least an hour, followed by acetone cleaning) through use of a hot melt press. It is required that the polymer be heated past its $T_g$ in order for it to adhere. The temperatures used for the lamination process were determined from the difference between the lamination ($T_l$) and the glass transition temperature ($T_g$) of the copolymer. As has been described in previous work, the best peel strength comes from a temperature range of $T_l - T_g = 100-150$ °C.[4] Greater temperatures than that cause the polymers to flow, while lower values lead to poor adhesion. The $T_g$'s measured by thermal mechanical analysis (TMA) are listed in Table 1. The values ranged from 160 to 190 °C. Hence, adhesion values were measured at lamination temperatures of 275 ± 10 and 300 ± 10 °C. The strips were laminated onto the alloy at these temperatures with 250 lb of pressure applied for 1 min, as was done previously.[4] The values for pressure and time of exposure have been chosen on the basis of optimum adhesion. The strips were then peeled off at room temperature at a 90° angle and a rate of 100 mm/min.

**Other Instrumentation.** All $T_g$'s and thermal expansion coefficients were measured by a Mettler TMA 40 thermal mechanical analyzer (TMA), with a Mettler TC 10A processor and a Mettler data acquisition system (Mettler Graphware TA 72PS.5). The temperature was scanned from 30 to 250 °C.

Gas chromatography was used to determine segment length distributions of the PDMS. This method was used in order to get an idea of what components were in the PDMS as well as the extent of overlap between different polymer distributions, not to obtain absolute molecular weight distributions, as the PDMS at higher molecular weights is not very volatile and the polymer may degrade. This will result in a distribution that is shifted toward lower molecular weights with a lower polydispersity index than is expected. To obtain more accurate distributions using GPC, the end groups of the PDMS must be derivatized as they will react with the column otherwise. The original chromatograms showed a nice evenly separated distribution. There appeared to be some contamination of cyclic silicones, particularly $Si_4O_4C_8H_{24}$ ($D_4$), in all samples. There was also some other form of non-amine-terminated PDMS present in the G-5 sample. It is important to remember that this PDMS will not react with the copolymer as it is not amine terminated and can be extracted. This further illustrates the importance of cleaning the surface with a nonpolar solvent such as toluene or hexane in order to extract this unreacted PDMS. The area under each peak was measured and plotted as a function of segment length to obtain a molecular weight distribution. A Hewlett-Packard 8890 gas chromatograph equipped with a 7673A autosampler and a flame ionization detector (FID) was employed. The detector was operated at 370 °C with He makeup gas flow of 30 mL/min. The ratio of hydrogen to air was set at 30/400 mL/min. The capillary column used was a J&W DB1-HT; 30 m × 0.25 mm i.d.; 0.1 $\mu$m film operated at 15 psi. The injector temperature was set at 275 °C. The initial temperature of the column was set at 70 °C for 1 min. The temperature was then ramped up to a final temperature of 360 °C at a rate of 10 °C/min. This temperature was maintained for 5 min in order to allow for peak elution. The carrier gas was He, which had a flow rate of approximately 1.0 mL/min at a temperature of 70 °C (15 psi). All gas chromatograms were taken by Occidental Chemical Corp.[39]

## Results and Discussion

**TMA Analysis.** The correlation between glass transition temperatures ($T_g$'s) and poly(imidesiloxane) composition is shown in Figure 1. As is shown in Figure 1a, there is a linear correlation between segment length and $T_g$. This linear behavior is attributed to the miscibility of the polymer. In miscible systems, $T_g$ typically varies monotonically as a function of composition, with a slight deviation from linearity.[40] The increase in $T_g$ with increasing segment length is attributed to the corresponding increase in the imide block length. Because of the increased domain sizes, the high-$T_g$ polyimide component is less susceptible to changes that result from the addition of the low-$T_g$ siloxane component. Figure 1b shows the effects of varying the siloxane composition in the polymer while maintaining a total weight percent of 10% siloxane. As the ratio of G-1 to G-9 increases, the $T_g$ decreases linearly. A similar effect is illustrated in Figure 1c with G-5 and G-9. This decrease in $T_g$ with increasing G-9 composition can be described in a similar manner as was discussed with Figure 1a. Longer segment lengths, and hence larger domain sizes, will lead to a decreased susceptibility to the addition of PDMS. It has also been shown that the $T_g$ decreases with increasing percentage of siloxanes although it is not shown here.[4] When more PDMS is added, there is not only an increase in the amount of low-$T_g$ component but a decrease in the size of the imide block as well. The coefficient of thermal expansion (CTE) of these polymers was measured as well (see Table 1). The values turned out to be around 100 ppm/K, which is consistent with the literature value.[4]

**XPS.** C 1s (285 eV), N 1s (402 eV), O 1s (531 eV), Si 2s (153 eV), and Si 2p (102 eV) peaks were detectable in all survey spectra taken. The peaks of interest, however, are that of the Si 2p peak, which comes from the PDMS component of the copolymer, and the N 1s peak, which comes from the hard segment or imide portion of the copolymer. The Si/N ratios will provide information about the extent of PDMS surface segregation. High-resolution XPS scans were taken at five different takeoff angles (10°, 15°, 30°, 45°, 90°), where the atomic concentrations of Si, C, N, and O were measured. The resultant Si/N ratios measured at 15° and 45° takeoff angles are plotted in Figure 2 as a function of increasing concentration of G-9. The error bars shown represent 1 standard deviation and are based on three measurements. Both cleaned and uncleaned samples are represented.

As is shown in Figure 2, the Si/N ratios are significantly lower for the samples cleaned in toluene at the 15° takeoff angle. This effect is less noticeable at the 45° angle, meaning that it is the topmost surface of the polymer that is being affected by the toluene treatment. IR spectra of the extract have confirmed that it is indeed PDMS that is being cleaned off the surface. The source of this could be unreated PDMS or $D_4$, which was found from GC analysis. It is also likely that nonstoichiometric

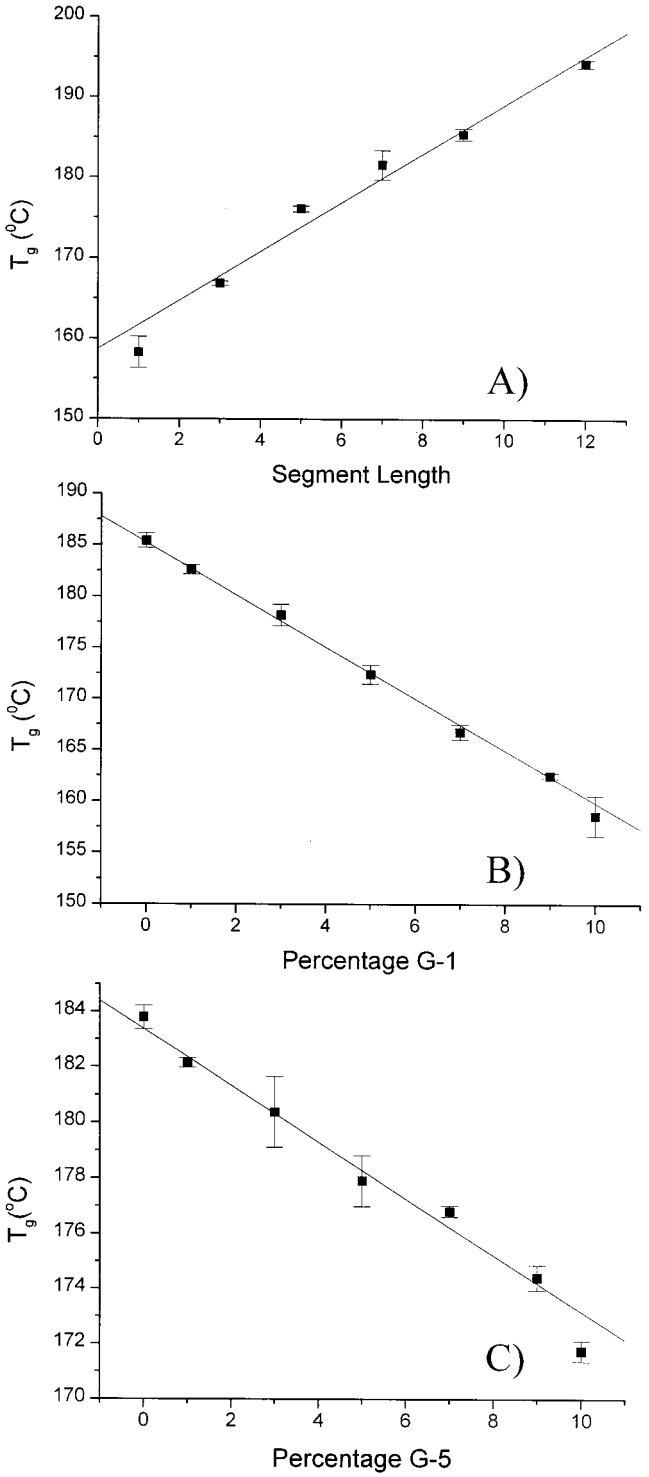


**Figure 1.** Glass transition temperatures plotted: (A) as a function of segment length ($R = -0.9892$, $m = 3.0318$, $b = 158.698$), (B) as a function of increasing G-1 content in a polymer comprised of both G-1 and G-9 (10% total siloxane) ($R = -0.999\,55$, $m = -2.5374$, $b = 185.24$), (C) as a function of increasing G-5 content in a polymer comprised of both G-5 and G-9 (10% total siloxane) ($R = -0.987\,86$, $m = -1.022$, $b = 183.38$). Note that these plots are linear.

PDMS rich low molecular weight polymer products would also be dissolved by the toluene. However, as was mentioned in the Experimental Section, it is extremely important that the unreacted or non-amine-terminated PDMS be extracted in order to minimize the contribution from the unreacted PDMS as well as stabilize the surface.

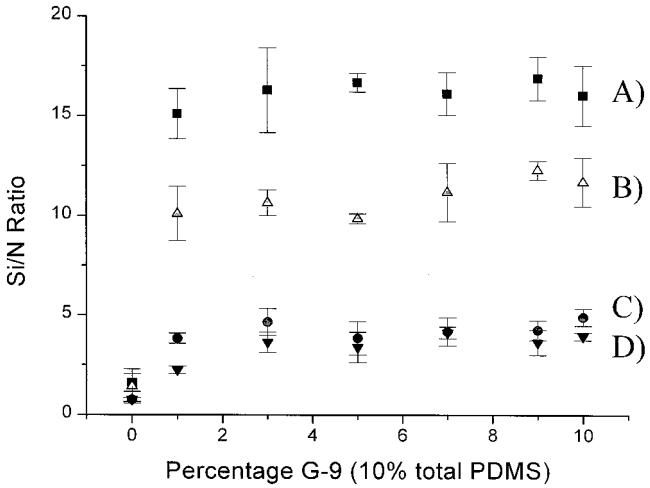


**Figure 2.** Si/N ratios of polymers comprised of both G-1 and G-9 as determined by high-resolution XPS. Values are plotted as a function of increasing G-9 percentage. Recall that the total composition is maintained at 10% PDMS. (A) (squares) 15° takeoff angle, (B) (triangles) 15° takeoff angle/sonicated in toluene for 2 min, (C) (circles) 45° takeoff angle, and (D) (upside-down triangles) 45° takeoff angle/sonicated in toluene for 2 min.

If there was no preferential segregation of certain PDMS segment lengths, it would be expected that the Si/N ratio would monotonically increase as the percentage of G-9 increases. However, this is not what is observed in Figure 2. Note that the pure G-1 polymer has a much lower Si/N ratio than does the remainder of this series. Yet, even with the addition of just 1% G-9, there is a drastic change in the Si/N ratio to a value that is statistically equivalent to that of the polymer containing 10% G-9 only. This illustrates that there is very little difference in the surface composition between polymers containing both G-9 and G-1 and the pure G-9 polymer, suggesting that there is preferential segregation of longer siloxane segment lengths to the surface in this polymer system. It should be mentioned here that the Si/N ratio of sample F, which is 1 wt % of G-9, also has a Si/N ratio that is comparable to polymers K−O. This segregation will be further confirmed by TOF-SIMS studies, which are currently underway.

This same process was carried out for the polymer series containing G-5 and G-9 ($W_a$−$W_e$). In this series, however, there is not much difference in the PDMS segment length distributions between G-5 and G-9, meaning that for the polymer comprised of G-9 only, there should be a considerable amount of G-5 and conversely with the polymer containing only G-5. Figure 3 shows the segment length/molecular weight distributions of both the G-5 and the G-9 as determined by GC.[38] These plots show that there is a significant amount of overlap between the two oligomer distributions. Hence, the driving force for segregation is not as great for the G-5/G-9 series as was the case with the G-1/G-9 series, and the effects of segregation according to length are expected to be less drastic.

Figure 4 shows the Si/N ratio of polymers H, Q, and $W_c$, containing 10% G-9, 10% G-5, and both 5% G-5 and 5% G-9, respectively. These ratios are plotted as a function of the sine of the photoelectric takeoff angle. (Figure 4a represents the Si/N ratios of the uncleaned samples, while Figure 4b depicts samples sonicated in toluene for 2 min.) The sample containing 5% G-5 and

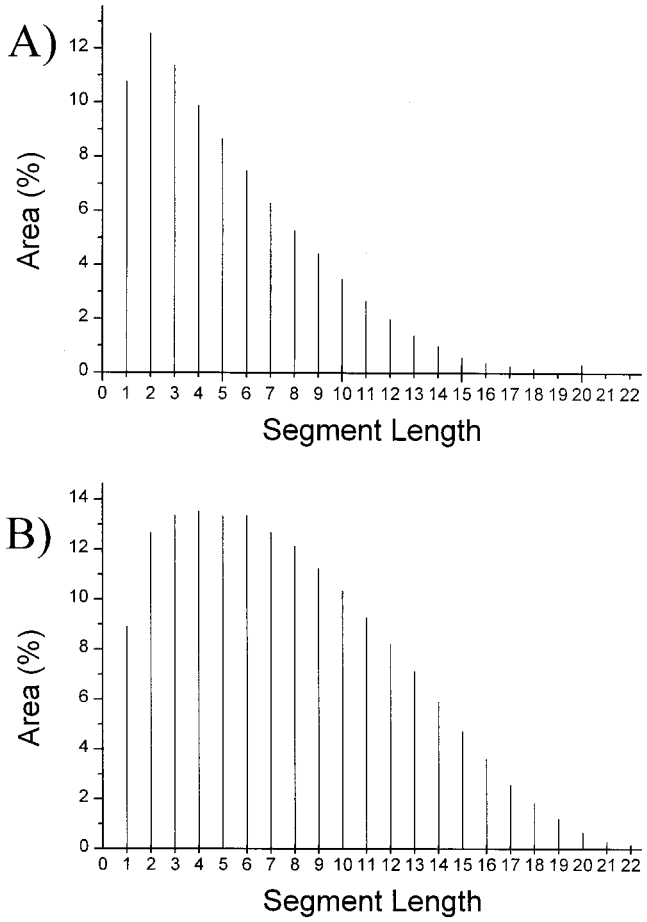


**Figure 3.** Segment length/molecular weight distributions as determined by GC: (A) G-5 distribution/$M_n$ = 564.23, $M_w$ = 685.66, and PDI = 1.22; (B) G-9 distribution/$M_n$ = 747.9, $M_w$ = 899.59, and PDI = 1.20. Chromatograms were measured by Occidental Chemical Corp. and have been recreated with permission.[38]

5% G-9 has a Si/N ratio that is intermediate to that of 10% G-9 and 10% G-5. However, this value is closer (within 2 standard deviations) to that of the 10% G-9 Si/N ratio than to that of the 10% G-5 (greater than 3 standard deviations away), which further confirms the possibility that there is preferential segregation of longer siloxane segments occurring. The decrease in the Si/N ratio as a result of cleaning with toluene is once again observed. The Si/N ratios of the G-5/G-9 series at takeoff angles of 15° and 45° were plotted vs increasing G-9 concentration in a similar manner as was done in Figure 2. The result is shown in Figure 5. Although the effect is not as great as the G-1/G-9 system, the surface compositions of this series containing varying percentages of G-5 and G-9 still more closely resemble that of the pure G-9 copolymer than the pure G-5 copolymer. However, at G-9 concentrations less than 3%, the Si/N ratio starts to skew toward that of the pure G-5 surface composition.

This preferential segregation of the longer siloxane chain lengths to the surface can be explained by end group effects. In a study done by Jalbert et al., changes in surface tension as a function of molecular weight of different types of PDMS are described.[41] It was found that, in samples where the end group of the PDMS had similar surface energies to the backbone, the surface tension did not change with molecular weight (e.g., −OH). However, with samples where the end group had

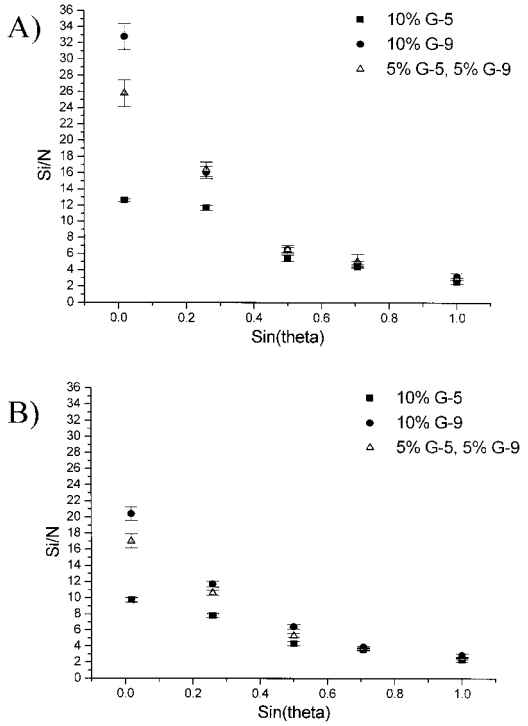


**Figure 4.** Si/N ratios as determined by high-resolution XPS, plotted as a function of the sine of the photoelectric takeoff angle. Squares represent polymers containing 10% G-5, circles represent 10% G-9, and triangles represent 5% G-5 and 5% G-9. (A) Untreated polymer; (B) sonicated in toluene for 2 min.

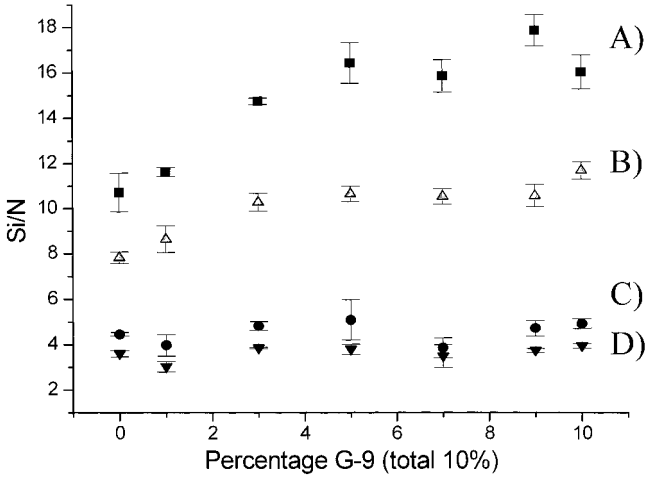


**Figure 5.** Si/N ratios of polymers comprised of both G-5 and G-9 as determined by high-resolution XPS. Values are plotted as a function of increasing G-9 percentage. Recall that the total composition is maintained at 10% PDMS. (A) (squares) 15° takeoff angle, (B) (triangles) 15° takeoff angle/sonicated in toluene for 2 min, (C) (circles) 45° takeoff angle, and (D) (upside-down triangles) 45° takeoff angle/sonicated in toluene for 2 min.

a surface energy that was greater than that of the backbone, the surface tension decreased with molecular weight (e.g., $-CH_2CH_2CH_2NH_2$). The opposite effect was observed for samples in which the end group had a lower surface energy than the polymer backbone (e.g., $-Si(CH_3)_3$). In our copolymers, if we consider the polyimide blocks analogous to the higher surface tension end group situation, then it would make sense that the higher molecular weight siloxanes are segregating to the surface in the system described here. Not only is there a lower surface tension associated with the longer chain

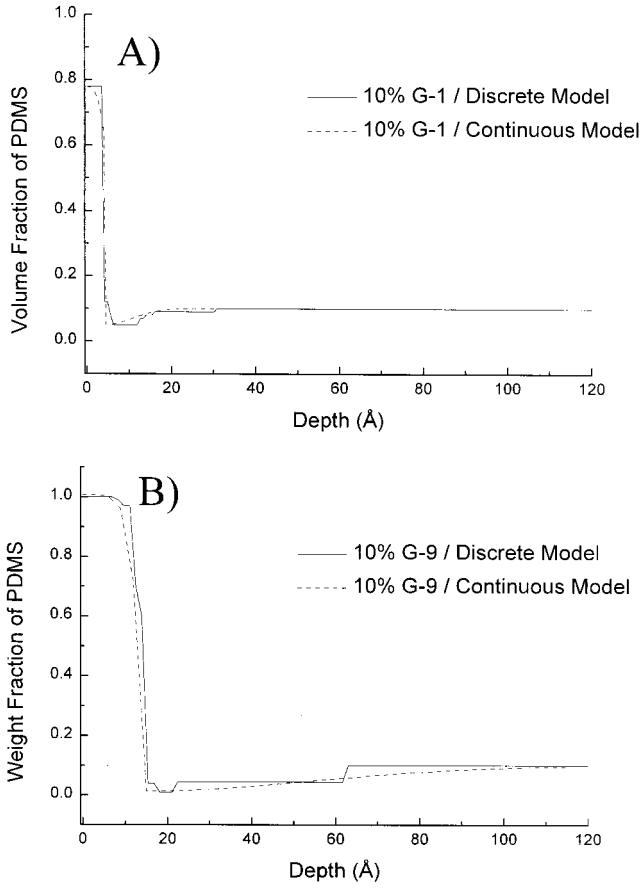


**Figure 6.** Deconvoluted concentration−depth profile, both discrete and continuous models for (A) sample C, containing only G-1, and (B) sample H, containing only G-9.

lengths, but a greater ability to bury the high surface energy imide groups at the ends of the chain.

**XPS Recovery of In-Depth Profile.** The calculated values for $C_{bulk}$, $\eta$, $\sigma$, and $\gamma$ are listed in Table 2. As is shown, the values used for samples K−O, which contain varying amounts of G-9 and G-1, are the same as that for pure G-9. Originally, the values that were used were averaged somewhere between G-1 and G-9 values, depending on the ratio of G-1/G-9. This was the only way to compensate for the different types of PDMS in the same polymer. However, the resultant depth profiles did not fit well with the experimental data. It resulted in profiles in which the surface composition was much greater than 100%. It also resulted in thicker siloxane-rich surface layers with increasing G-1 content. This did not make sense. The greater the percentage of G-1 that was in the polymer, the greater was the observed error due to the changing values of $\eta$, $\sigma$, and $\gamma$. Our interpretation was that since the surface was comprised primarily of G-9, and the Si signal obtained by XPS originated from G-9 only, using averages for $\eta$, $\sigma$, and $\gamma$ based on both G-1 and G-9 would not be effective in obtaining accurate profile information.

The resultant depth profiles for G-1 and G-9 are depicted in Figure 6. The solid lines represent the discrete model, while the dashed lines are the results from the continuous model. Recall that the purpose of the discrete model is to determine a curve shape which best fits the experimental data. The profile of C represented by Figure 6a resulted in C/Si ratios of 13.02, 19.98, 24.81, and 30.12 for 15°, 30°, 45°, and 90°, respectively, for the discrete model. The actual experimental values were 13.07 ± 2.28, 20.02 ± 1.58, 23.59 ± 2.36, and 30.18 ± 2.43. For sample H shown in Figure 6b, the values were 3.13, 4.60, 6.01, and 7.94 for the discrete model, while the actual experimental values were 3.11 ± 0.21, 4.49 ± 0.28, 5.96 ± 0.49, and 8.15 ± 0.29. As can be seen, the values calculated by the discrete model are within experimental error. The continuous model was then defined on the basis of the results of the discrete model calculations. The parameters used in this model and the resultant error ($\Psi$) are listed in Table 2. It is obvious that the greater the amount of error in the experimental data, the greater will be the error in the depth profile. In fact, because of the ill-posed nature of eqs 5 and 6 (solution to equations requires a matrix inversion for which no unique solution exists), small variations in the photoelectron intensities and other algorithm parameters may result in very different depth profiles.[42] However, setting boundary conditions based on the polymer compositions will limit the variability.

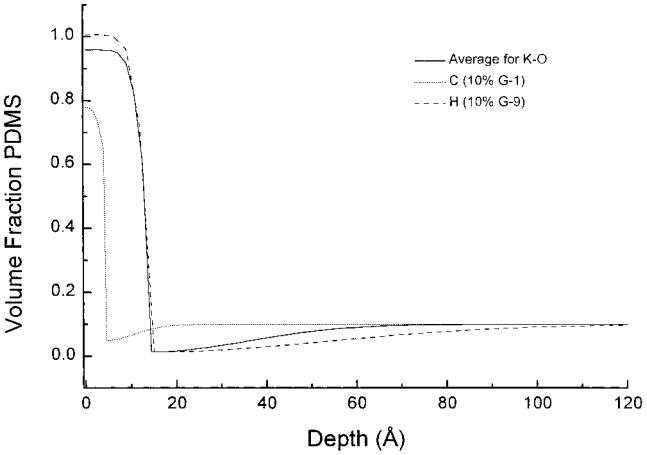


**Figure 7.** Deconvoluted concentration−depth profile of samples C (10% G-1), H (10% G-9), and polymers K−O (varying amounts of G-1 and G-9).

Figure 7 shows the final profiles for all samples including samples K−O. Since the C/Si ratios of all samples K−O were statistically equivalent, an average was taken at all four angles, and an average profile was taken. Note that the amount of error ($\Psi$) for polymers K−O is much less than that of polymer C or H. This is most likely because there are five samples (15 measurements) being averaged together to obtain a result. As a result, the C/Si ratios are much more accurate than the profiles obtained with H and C in which only three measurements were taken. In fact, the curves represented by H and polymers K−O are within experimental error, as their C-to-Si ratios were found to be statistically equivalent at every angle. They are depicted in this manner in order to illustrate that the curves are similar. In other words, the surfaces of all polymers containing any amount of G-9 were found to be the same. No amount of G-1 resulted in a change in the profile.

Note the shape of the profiles. Immediately following the sharp drop-off of siloxane in the curve is a depletion layer, in which the amount of siloxane is below the bulk value. This feature is common in polymer systems such as this and has been described in detail in previous papers.[24] There are four primary features that are important in the interpretation of these profiles. The height of the plateau gives information on the surface content of PDMS. According to the profiles shown, the

**Table 3. Correlaton between the Thickness of the Surface PDMS-Rich Layer Poly(imidesiloxane) and the Calculated PDMS Chain Dimensions Using Various Models**

| polymer | free jointed chain model (Å) | short-range effects model ($\phi = 143°$) (Å) | short-range effects model ($\phi = 110°$) (Å) | exptl value (Å) |
|---|---|---|---|---|
| C/10% G-1 only | 2.3 | 6.9 | 3.3 | 4.5 |
| H/10% G-9 only | 7.0 | 20.8 | 9.9 | 14.2 |
| K−O/polymer mixtures (av) | | | | 14.7 |

surface concentration of PDMS for sample H is 101 ± 3%, meaning that the surface is comprised of pure PDMS at the limits of detection of XPS. The surface concentrations determined for polymers K−O according to the depth profiles turned out to be 96 ± 3%. These two values are within experimental error, which further proves that there is no difference between the polymers containing G-1 and the pure G-9. Sample C however had a much lower value of 78% total surface PDMS. These data further confirm that the extent of PDMS segregation is extremely sensitive to the length of the incorporated siloxane segment.

The depth of the trough tells us how much polyimide there is in the depletion layer, while the width will tell us how thick the depletion layer is. It can be seen upon comparison of the widths and depths of the troughs that there is a much smaller depletion layer in polymer C, containing only G-1, as compared to any of the other polymers. This can also be attributed to the size of the segment length. Recall that decreasing the block length of the PDMS portion of the polymer will also result in a decreased block length of the imide length if the overall percentage is to be maintained at 10%. Hence, the block length of the imide will be shorter as a result of having a shorter siloxane length and the depletion layer will be decreased. It should be noted here, however, that the greatest amount of irreproducibility appeared in this portion of the profile (e.g., the values varied greatly from spectra to spectra). This can be attributed to the error due to signal from deeper sampling depths. The contribution of signal from lower layers is small at high takeoff angles, even though the total signal is constant. Since there is a decrease in the amount of signal reaching the detector from greater depths, and therefore a lower signal-to-noise ratio at greater sampling depths, it can be expected that the profile should be less precise with increasing depth.

The location of the trough gives information on the thickness of the siloxane surface layer. Table 3 shows the thickness (±0.3 Å) of the PDMS surface layer as determined by the deconvolution process as compared to theoretical chain dimensions.[24] The theoretical values were calculated using two different models: the free jointed chain model and the short-range effects model. The freely jointed chain model assumes no restrictions, while the more realistic short-range effects model accounts for restrictions due to bond angle. There are two different bond angles in PDMS: the Si−O−Si, which has an angle of ∼143°, and O−Si−O, with an angle of ∼110°.[24] The bond length of the Si−O bond is 1.64 Å.[24] The experimental values for thickness, as shown in Table 3, are almost directly between the two values of the short-range effects model. This makes sense, since the PDMS contains 50% Si−O−Si and 50% O−Si−O bond angles. These values are much higher than has been determined previously[24] (4.4 Å for G-1 and 8.6 Å for G-9), most likely as a result of the increased heating time in the cure process as well as modifications in the calculation and fits that were described in the Experimental Section, including using C/Si rather than C/N ratios, and the addition of the *y* exponent. These modifications result in data that better match with the theoretical models than our previous efforts. It is also important to note that, in agreement with the previous results, the freely jointed chain model starts to play a greater role in the longer chain polymers.[24] That is why the value for G-9 is slightly skewed toward the value represented by the freely jointed chain.

**Adhesion Studies.** The final stage of this study was to relate the surface properties determined from XPS of this polymer series to the adhesion. Figure 8 shows the adhesion values of these polymers as measured by peel strength testing at two different temperatures. As can be seen, the peel strengths of all polymers, except for the pure G-1, have similar adhesion values. This is consistent with the results found by XPS. Sample C, containing pure G-1, which was found by XPS to have the highest amount of imide near the surface, had the greatest adhesion strength. The remainder of the samples containing varying amounts of G-9 had similar surface compositions, no matter what the ratio of G-9 to G-1, resulting in statistically equivalent adhesion strengths. The adhesion strengths of the series are much lower than that of the pure G-1 copolymer simply because there is a greater concentration of PDMS at the surface and a thicker PDMS surface layer as was previously discussed. This limits the interaction of the imide with the surface of the steel.

The effect of cleaning the polymer surfaces on the adhesion characteristics was also examined. These results are depicted in Figure 8b. It is obvious that the samples which were sonicated in toluene have higher adhesion strengths, most likely associated with the removal of excess unreacted PDMS from the surface, which could form a weak boundary layer. This result correlates well with the XPS findings in which the Si/N ratio decreased after toluene treatment. In Figure 8c, the adhesion of the samples was measured again, except in this case all of the samples were cleaned with toluene and dried before the adhesion was measured. The temperature of the hot press had to be lowered in order to measure the adhesion strengths because at 300 °C the adhesion was too high and was difficult to measure accurately. That is the reason for the missing G-1 value in Figure 8b.

Figure 9 shows the peel strength tests performed for the G-5/G-9 series at 275 °C for 1 min at 250 lb pressure. The effects of toluene treatment are obvious in this graph as the adhesion values are significantly greater than that of the untreated samples. The important thing to notice in this study however is that there is no significant difference in the adhesion strengths between any of these polymers. This is expected as the differences in the surface compositions are slight. These results are consistent with previous findings.[24] One oddity, however, is that the overall adhesion strength of this series as compared to that of the G-1/G-9 polymer series was greater. However, it is the relative adhesion values that are of interest, and sample H, which is a part of both series, can be thought of as a control. This

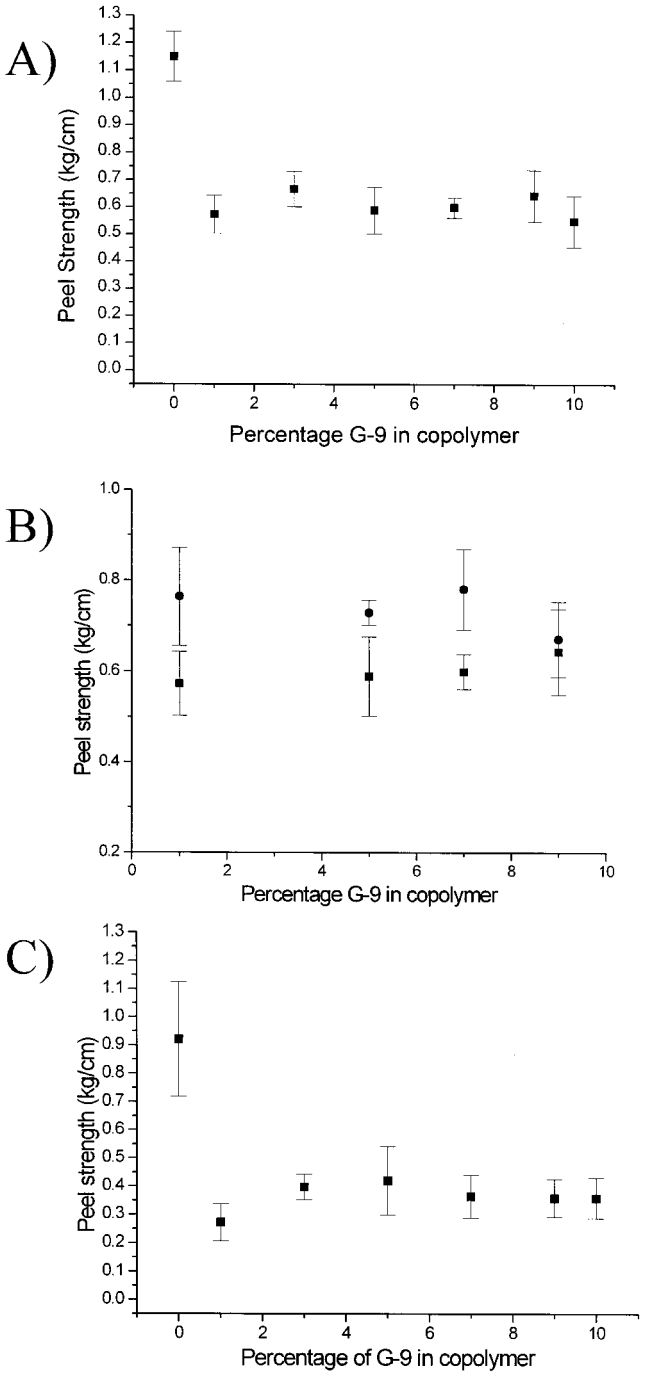


**Figure 8.** Correlation between the adhesion as measured by peel strength (kg/cm) and the percentage of G-9 in polymers comprised of both G-1 and G-9. (A) Placed in hot press for 1 min at 300 °C and 250 lb pressure. (B) Placed in hot press for 1 min at 300 °C and 250 lb pressure. Squares represent nontreated samples, while circles represent samples sonicated in toluene for 5 min. [Note: not all polymers were measured as the adhesion was too high]. (C) Placed in hot press for 1 min at 275 °C and 250 lb pressure/sonicated in toluene for 5 min.

type of variability in peel strength testing is a common occurrence. There is also some slight variability in the sample preparation as can be seen with the measurement of the $T_g$ (see Figure 1).

## Conclusions

A series of poly(imidesiloxanes) containing multiple siloxane segment lengths in a single polymer have been synthesized. In our studies, the ratio of G-9 to G-1 in poly(imidesiloxane) copolymers was varied at a constant overall siloxane composition of 10%. It was found that the surface composition of polymers containing both G-1 and G-9 was not significantly different from that of the polymer which contained G-9 only. However, the pure G-1 sample had a much lower Si/N ratio. The same experiments were carried out for samples in which the ratio of G-9 to G-5 was varied. Since these segment lengths have molecular weight distributions that overlap, the effect was not as pronounced. However, the composition at the surface of samples containing both G-5 and G-9 was closer to that of the sample comprised of G-9 only than that of the sample containing pure G-5. These results suggest the preferential segregation of longer siloxane segment lengths to the surface in the copolymer system described in this paper. The preferential segregation is most likely due to the end group effects of the high surface energy imide groups. To minimize the total free energy of the system, it is favorable to minimize the interactions of the imide portion with the surface. It is much easier to do this with longer segment lengths. Upon sonication with toluene, the Si/N ratios as measured by XPS decreased significantly, most likely because of the removal of unreacted PDMS from the surface.

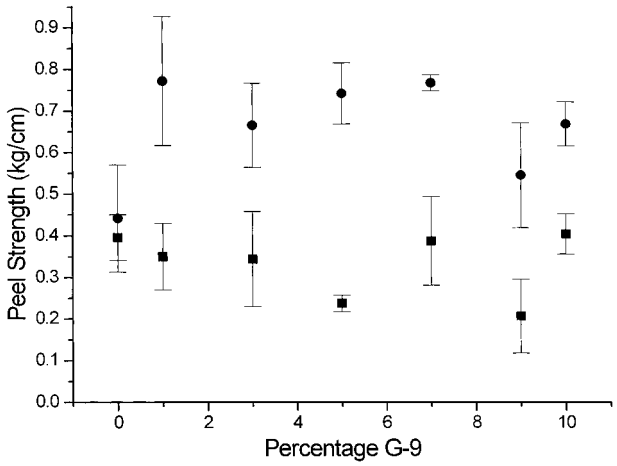


**Figure 9.** Correlation between the adhesion as measured by peel strength (kg/cm) and the percentage of G-9 in polymers comprised of both G-5 and G-9. Samples placed in hot press for 1 min at 275 °C and 250 lb pressure. Squares represent nontreated samples. Circles represent samples sonicated in toluene for 5 min.

The XPS data were used to obtain depth information by following a series of steps involving the convolution of a theoretical profile based on known polymer compositions. It was found that the thickness of the surface-rich PDMS layer was the same for all polymers containing G-9, no matter what the ratio. The actual values for the surface layer thickness agree with theoretical chain dimensions.

The adhesion studies correlated well with the XPS results. The adhesion strengths of the mixed polymers were about the same as that of the polymer containing pure G-9, while that of the pure G-1 was significantly higher. The increased adhesion of the sample containing pure G-1 is associated with a thinner PDMS boundry layer, while the decreased adhesion in the rest of the samples is attributed to thicker PDMS layers. The increase in adhesion upon toluene treatment was a result of the loss of excess PDMS from the surface as was verified by the decreasing Si/N ratios in XPS.

**Acknowledgment.** This research was supported in part by the Office of Naval Research and the National Science Foundation. We also acknowledge Dr. Sergio Rojstaczer from Kulicke and Soffa Industries for his help with polymer synthesis.

## References and Notes

(1) Lupinski, J. H.; Moore, R. S. *ACS Symp. Ser.* **1988**, *407*, 1.
(2) Homma, T.; Yamaguchi, M.; Kutsuzawa, Y.; Otsuka, N. *Thin Solid Films* **1999**, *28*, 237.
(3) Hedrick, J. L.; Brown, H. R.; Volksen, W.; Sanchez, M.; Plummer, C. J. G.; Hilborn, J. G. *Polymer* **1987**, *38*, 605.
(4) Rosenfeld, J.; Acharya, H. R.; Choi, J.-O.; Suzuki, T. In *Poly-(imide siloxanes)s*; Salamone, J. C., Ed., CRC Press: Boca Raton, FL, 1996; p 6198.
(5) Furukawa, N.; Yamada, Y.; Furukawa, M.; Yuasa, M.; Kimura, Y. *J. Polym. Sci., Part A: Polym. Chem.* **1997**, *35*, 2239.
(6) Chen, J.; Gardella, J. A., Jr. *Appl. Spectrosc.* **1998**, *52*, 361.
(7) Chen, J.; Gardella, J. A., Jr. *Macromolecules* **1998**, *31*, 9328.
(8) Chen, X.; Gardella, J. A., Jr. *Macromolecules* **1994**, *27*, 3363.
(9) Zhuang, H.; Gardella, J. A., Jr. *Macromolecules* **1997**, *30*, 3632.
(10) Chen, X.; Lee, H. F.; Gardella, J. A., Jr. *Macromolecules* **1993**, *26*, 4601.
(11) Schmitt, R. L.; Gardella, J. A., Jr.; Magill, J. H.; Salvati, L.; Chin, R. L. *Macromolecules* **1985**, *18*, 2675.
(12) Mittlefehldt, E. R.; Gardella, J. A., Jr. *Appl. Spectrosc.* **1989**, *43*, 1172.
(13) Smith, S. D.; DeSimone, J. M.; Huang, H.; York, G.; Dwight, D. W.; Wilkes, G. L.; McGrath, J. E. *Macromolecules* **1992**, *25*, 2575.
(14) Chen, X.; Cohen, R. E.; Gardella, J. A., Jr. *Macromolecules* **1994**, *27*, 2206.
(15) Zhuang, H.-Z.; Hercules, D. M.; Gardella, J. A., Jr. *Macromolecules* **1997**, *30*, 1153.
(16) Chen, X.; Ho, T.; Wynne, K. J.; Gardella, J. A., Jr. *Macromolecules* **1995**, *28*, 1635.
(17) Chen, X.; Gardella, J. A., Jr.; Kumler, P. L. *Macromolecules* **1993**, *26*, 3778.
(18) Li, L.; Chan, C.; Wen, L. T. *Macromolecules* **1997**, *30*, 3698.
(19) Patel, N. M.; Dwight, D. W.; Hedrick, J. L.; Webster, D. C.; McGrath, J. E. *Macromolecules* **1988**, *21*, 2689.
(20) Schmitt, R. L.; Gardella, J. A., Jr.; Magill, J. H.; Chin, R. L. *Polymer* **1987**, *28*, 1467.
(21) Spontak, R. J.; Williams, M. C. *J. Appl. Polym. Sci.* **1989**, *38*, 1607.
(22) Spontak, R. J.; Williams, M. C. *Polym. J.* **1988**, *20*, 649.
(23) Zhao, J.; Rojstaczer, S. R.; Gardella, J. A., Jr. *J. Vac. Sci. Technol. A* **1998**, *16*, 3046.
(24) Zhao, J.; Rojstaczer, S. R.; Chen, J.; Xu, M.; Gardella, J. A., Jr. *Macromolecules* **1999**, *32*, 455.
(25) Zuang, H.-Z.; Gardella, J. A., Jr.; Incavo, J. A.; Rojstaczer, S. R.; Rosenfeld, J. C. *J. Adhes.* **1997**, *63*, 199.
(26) Yoon, T. H.; Arnold-McKenna, C. A.; McGrath, J. E. *J. Adhes.* **1992**, *39*, 15.
(27) Chen, K.-M.; Ho, S.-M.; Wang, T.-H.; King, J.-S.; Chang, W.-C.; Cheng, R. P.; Hung, A. *J. Appl. Polym. Sci.* **1992**, *45*, 947.
(28) Nakumura, Y.; Suzuki, Y.; Watanabe, Y. *Thin Solid Films* **1996**, *290*−*291*, 367.
(29) Park, I. S.; Yu, J. *Acta Mater.* **1998**, *46*, 2947.
(30) Rojstaczer, S. R. U.S. Pat. 5,209,981.
(31) Rojstaczer, S. R.; Tang, D. Y.; Tyrell, J. A. U.S. Pat. 5,317,-049.
(32) Lee, C. J. U.S. Pat. 4,973,645.
(33) *Handbook of X-ray Photoelectron Spectroscopy*; Perkin-Elmer Corp.: Norwalk, CT, 1979.
(34) Vargo, T. G.; Gardella, J. A., Jr. *J. Vac. Sci. Technol.* **1989**, *A7*, 1733.
(35) Gardella, J. A., Jr.; Wynne, K. J.; McCarthy, T. J.; Rabolt, J. F.; Belfort, G. *Naval Research Reviews, Special Issue on Biofouling*; Wynne, K. J., Guard, H., Eds.; **1997**, *XLIX* (4), 19−34.
(36) Zhuang, H.-Z.; Gribben-Marra, K.; Ho, T.; Chapman, T. M.; Gardella, J. A., Jr. *Macromolecules* **1996**, *29*, 1660.
(37) Gardella, J. A., Jr.; Ho, T.; Wynne, K. J.; Zhuang, H.-Z. *J. Colloid Interface Sci.* **1995**, *176*, 277.
(38) Tanuma, S.; Powell, C. J.; Penn, D. R. *Surf. Interface Anal.* **1993**, *20*, 77.
(39) Domroes, D.; Ruzaj, M.; Rosenfeld, J., unpublished results (Occidental Chemical Corp.).
(40) Burkhardt, C. A.; Gardella, J. A., Jr. *Appl. Spectrosc.* **1993**, *47*, 1636.
(41) Jalbert, C.; Koberstein, J. T.; Yilgor, I.; Gallagher, P.; Krukonis, V. *Macromolecules* **1993**, *26*, 3069.
(42) Tielsch, B. J.; Fulgham, J. E. *Surf. Interface Anal.* **1994**, *21*, 621.

MA010353Y